

Observation and Simulation of the Transient Anion Oligomers $(\text{LiClO}_4)_n^-$ ($n = 1 - 4$) in Diethyl Carbonate LiClO₄ Solutions

Furong Wang,^Φ Pascal Pernot,^Φ Pierre Archirel,^Φ Daniel Ortiz[†], Sophie Le Caër,[†] and Mehran Mostafavi^{Φ*}

^Φ Laboratoire de Chimie-Physique/ELYSE, UMR 8000 CNRS/UPS, Université Paris Sud, Bât. 349, F-91405 Orsay Cedex, France.

[†] LIONS, NIMBE, UMR 3685, CEA, CNRS, Université Paris-Saclay, CEA Saclay Bât. 546, F-91191 Gif-sur-Yvette Cedex, France.

*Corresponding author, email: mehran.mostafavi@u-psud.fr

Abstract

NMR measurements show that diethyl carbonate (DEC, a solvent with a low dielectric constant) solutions of LiClO₄ contain $(\text{LiClO}_4)_n$ oligomers. The reduction of these species by solvated electrons and pre-solvated electrons is followed by picosecond pulse radiolysis measurements. The data analysis shows that several anions absorbing in the NIR and visible range are formed after the 7 ps electron pulse. In contrast with THF solutions of LiClO₄, the anionic monomer $(\text{LiClO}_4)^-$ is not observed in DEC solutions. This is due to the fact that DEC is a non-polar solvent favoring the clustering of the monomers in the non-irradiated solution as shown by NMR results, and also due to the instability of the anionic monomer. The absorption spectra of the anionic dimer $(\text{LiClO}_4)_2^-$, trimer $(\text{LiClO}_4)_3^-$ and tetramer $(\text{LiClO}_4)_4^-$ are clearly observed in NIR and in visible ranges. Compared to the results obtained for the same system in THF, and in agreement with simulated absorption spectra, the experimental results show that the absorption bands are shifted to the blue when n increases. The kinetics recorded for the molar LiClO₄ solution indicate that the solute is only under the form of oligomers $(\text{LiClO}_4)_n$ with a large n value and that the reduced species absorb weakly in the visible. Lastly, and contrarily to what is known for well separated ions in polar solvents, it is shown that the $(\text{LiClO}_4)_n^-$ anions are not stable with respect to self-reduction, leading to the decomposition of perchlorate anions. In this reaction the perchlorate anion ClO₄⁻ is reduced by the Li atom into a chlorate anion ClO₃⁻. This is proved by the presence of ClO₃⁻ and of chlorinated species detected by mass spectrometry measurements in irradiated DEC solutions containing LiClO₄.

Introduction

The solvated electron formed in a variety of solvents has an intense optical absorption band and can be used as a reducing agent to follow the chemical reactivity of many compounds in liquids.¹⁻⁸ In water, the hydrated electron is considered to be a strong reducer of metal ions except for earth alkaline (M^{2+}) and alkaline (M^+) metal ions.⁷ In these latter cases, ion pairings (M^+ , e_{aq}^-), characterized by a blue shift of the absorption band as compared to the band of the hydrated electron in neat water, are observed. For a given concentration, the amplitude of this band shift depends on the cation charge.⁹ This trend was also reported in low polarity solvents. In ethers, such as tetrahydrofuran (THF, $\epsilon_s = 7.4$), it is known that for a dilute solution of metal cations, the maximum of the absorption band of e_s^- , located at 2200 nm, shifts significantly towards 890 nm in the presence of sodium salts.¹⁰ The formation of (M^+ , e_s^-) pairs, observed by microsecond pulse radiolysis, was also supported by ESR measurements in the case of Na^+ , showing that a “monomeric” neutral species is formed between e_s^- and M^+ .¹¹ These studies were all performed in dilute solution of metal cations for which M^+ is not associated with its counter ion. However, for concentrated solutions of alkaline and earth alkaline metal ions, the situation can be markedly different. To investigate the formation of transient species in more concentrated solutions of non-reactive metal cations, picosecond pulse radiolysis measurements of THF solutions containing decimolar $LiClO_4$ were recently performed.¹² It was concluded that the solvated electron scavenger is not the dissociated metal cation but the salt or even several oligomers of the salt $(LiClO_4)_n$ which are present in solution and react with the solvated electron to form $(LiClO_4)_n^-$ anions. The absorption bands of the anionic monomer $(LiClO_4)^-$, dimer $(LiClO_4)_2^-$, trimer $(LiClO_4)_3^-$ and tetramer $(LiClO_4)_4^-$ in THF were obtained by molecular simulations.¹² The simulations evidenced also that the Li^+ ion becomes reactive when the electron is scavenged by $LiClO_4$ and catalyses the reduction of perchlorate by excess electrons. However, no experimental proof was reported for that statement.

In the present work, the kinetics of the reaction between the solvated electron and $LiClO_4$ are investigated in diethyl carbonate (DEC, $C_2H_5OCOOC_2H_5$) chosen for two main reasons: first, its polarity is very low ($\epsilon_s = 2.8$), even lower than that of THF ($\epsilon_s = 7.4$); second, DEC is used in Li-ion batteries as a co-solvent with other carbonates and Li^+ ions play the role of charge transporter in these batteries. Therefore, in this solvent, it is interesting to investigate the reactivity of the salt by following the decay of the solvated electron by the picosecond pulse radiolysis method and the observation of the transient species.^{13,14} Here, transient spectra in a large spectral window from 400 to 1450 nm are measured, and the effects of the concentration of the salt from 0.05 up to 1 mol L⁻¹, which corresponds to the Li^+ concentration in Li-batteries, are studied. Theoretical calculations are also performed to identify the species responsible for these transient absorption spectra. The simulated absorption spectra of the products are compared with experimental data. Finally, the results are compared with those obtained in THF and water and the role of Li^+ as a catalyst reducing the ClO_4^- counter ion is

investigated by high-resolution mass spectrometry (HRMS) measurements of the products obtained in the same solutions after irradiation.

Experimental and theoretical section

Chemicals. The purity of DEC solvent and of dry LiClO₄ was 99% and 99.99% respectively, and they were used as received from Sigma-Aldrich. To avoid any water uptake, LiClO₄ was dissolved in DEC using a glove bag under argon atmosphere.

NMR measurements. In order to describe the nature of species present in DEC/LiClO₄ solutions, ³⁵Cl nuclear magnetic resonance experiments (NMR) were recorded on a Bruker Avance I 400, with a 5 mm BBO probe, at 39 MHz. The NMR parameters were a spectral width of 40 kHz, 32 K data points for the time domain, a 0.4 s acquisition time, a recycle time of 0.1 s and an accumulation of 300 scans. Chemical shifts were reported with reference to ³⁵Cl in a solution of NaCl in D₂O.

Mass spectrometry experiments. For the detection of the stable products formed in the liquid phase, DEC/LiClO₄ solutions were irradiated in ampoules under argon atmosphere using 10 MeV electron pulses of a Titan Beta, Inc. linear accelerator (LINAC). The duration of the pulse was 10 ns and the repetition rate was set to 2 Hz in order to avoid any macroscopic heating of the sample during irradiation. The dose per pulse ($30 \pm 2 \text{ Gy.pulse}^{-1}$) was determined using the Fricke dosimetry¹⁵ and the total dose received by the system was 100 kGy. High-resolution mass spectrometry (HRMS) experiments of the irradiated and non-irradiated solutions were then recorded in both positive and negative modes using Electrospray Ionization (ESI) coupled to a Fourier Transform Ion Cyclotron Resonance Spectrometer (Bruker FT-ICR, 7 T). The solutions were prepared by mixing 100 µL of the DEC/LiClO₄ solution with a) 1 mL of H₂O/MeOH (40:60) and 2 µL of formic acid and b) MeOH /acetonitrile (50:50) and 2 µL of formic acid. All solutions were infused with a syringe pump at a flow of 5 µL min⁻¹ and their ionization was achieved by applying a voltage of 5.5 kV on the sprayer probe.

Picosecond pulse radiolysis set-up. The experimental study was performed using the ELYSE laser-induced electron accelerator. The pulses are of 3-5 nC, 5-10 ps, with an electron energy of 6-8 MeV, at a repetition frequency of 10 Hz.^{16,17} The transient absorbance was measured with a broadband pump-probe detection device, whose principle was already described elsewhere.¹⁸ In the visible range, a transient absorbance due to the fused silica cell windows was detected in the empty cell when irradiated,¹⁹ and was subtracted from the absorbance data of the cell containing the DEC solutions.

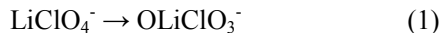
The broadband pump-probe system was operated in two configurations, one for the visible using a single crystal of CaF₂ for continuum light generation, one using a single crystal of yttrium aluminum garnet (YAG) for continuum light generation optimized on the near Infrared (NIR). Probe and reference beams were each coupled into an optical fiber, transmitted to an adapted spectrometer, and dispersed onto the specific line scan detectors. For the measurements in the NIR, a customized

broadband polychromator with an InGaAs photodiode array from Hamamatsu (G11608-512DA) was used.²⁰ Thanks to the new development and particularly to the enhanced response down to the visible, spectral overlap of both detection configurations was achieved in the region below the fundamental laser wavelength of 780 nm. The optical path of the flow cell is 0.5 cm. The time resolution is 15 ps (the pulse width of the electron pulse being around 7 ps). The dose per pulse is deduced from the absorbance of the hydrated electron e^-_{aq} in water, measured just before a series of experiments in DEC solutions. The dose was then derived from the yield at 10 ps²¹: $G(e^-_{aq})_{10\text{ps}} = 4.25 \times 10^{-7} \text{ mol J}^{-1}$ and from the solvated electron molar absorption coefficient $\epsilon_{\lambda=600\text{ nm}} = 1.33 \times 10^4 \text{ L mol}^{-1} \text{ cm}^{-1}$. The dose per pulse in water was typically around $D = 48 \text{ Gy}$.

Spectro-kinetic data analysis. The data matrices resulted from the averaging of about 30 scans, after removal of singular points arising from outlier laser shots.¹² They were then corrected for a wavelength-dependent baseline in order to be analyzed by a multivariate curve resolution alternating least squares (MCR-ALS) approach.^{22,23} The number of absorbing species in a global matrix was assessed by Singular Value Decomposition (SVD)²⁴ of the global matrix, and a MCR-ALS analysis with the corresponding number of species was performed. Positivity constraints were imposed for both spectra and kinetics. The residual maps were systematically inspected to assess the absence of model defects. The corresponding MCR-ALS code was adapted from the ALS package by K.M. Mullen.²⁵

Simulations. In a recent article, we have explained in details molecular simulations of the structure and the absorption bands of the oligomer anions $(\text{LiClO}_4)_n^-$ ($n = 1-4$) in solution in THF.¹² These simulations were based upon a classical MC (Monte-Carlo) sampling of the nuclear configurations with the GIBBS code,²⁶ a quantum DFT (Density Functional Theory) treatment of the electrons and a classical modeling of the solvent with the SMD (Solvation Model using Density) formalism.²⁷ The absorption spectra are a convolution of the TDDFT lines of a sub-list of the MC configurations with a Gaussian function and $\text{fwhm} = 0.2 \text{ eV}$. All the DFT calculations had been performed with the Gaussian 09 package.²⁸ The same methodology was applied in the present work for the calculations of the oligomer anions in DEC.

As reported in this work, the simulations are actually difficult because all the anions of interest are metastable with respect to the self-reduction reaction, *i.e.* for the monomer:¹²



In this reaction the perchlorate anion ClO_4^- is reduced by the Li atom into a chlorate anion ClO_3^- . This reaction displays in THF a free energy change of -2.58 eV at the B3LYP level, and a barrier free energy of + 0.53 eV at the MPW1K level. We could establish that:¹²

1. The B3LYP functional²⁹ is a good one as far as absorption spectra are calculated, but is not usable for the molecular simulations, because the ClO bond breaking due to reaction (1) occurs at the very

beginning of the simulation. Only the anion dimer $(\text{LiClO}_4)_2^-$ proves to be stable a long enough time at the B3LYP level for the absorption spectrum to be reliably calculated.

2. The MPW1K functional³⁰ fixes the ClO bond breaking issues and enables MC simulations with an acceptable number of MC steps (10 000 for the monomer, 20 000 for the trimer and tetramer).
3. The MPW1K MC configurations may be modified in a simple way (stretching of all the ClO distances by 2.6%), so as to enable the B3LYP calculation of the absorption spectrum. For this reason, we call our method the hybrid MPW1K/B3LYP simulation method.

The MC simulations of the oligomer anions $n = 1-4$ were performed with this method and an excellent agreement was found with the experimental results. The simulations also gave the different structures of the oligomers anions.

Results

Solute structure in concentrated solutions of lithium perchlorate in DEC. Before reporting the results of the pulse radiolysis measurements, it is important to characterize the species present in the diethyl carbonate (DEC) solutions at room temperature. DEC is a solvent with a very low static dielectric constant ($\epsilon_s = 2.8$). It is known that ionic salts are weakly dissociated in this kind of solvents. For example, it was reported in the case of LiClO_4 in diethyl ether solutions (with a static dielectric constant of 4.3) that all the lithium perchlorates are in the form of contact ion pairs at a concentration of 0.1 mol L^{-1} .³¹ Moreover, no evidence of the presence of isolated perchlorate ions was found at this concentration. The presence of noticeable neutral clusters $(\text{LiClO}_4)_n$ with $n > 1$ was detected at concentrations greater than 0.2 mol L^{-1} in diethyl ether. For instance, at 0.5 mol L^{-1} concentration (resp. 1 mol L^{-1}), it was concluded that 90 % (resp. 82%) of lithium perchlorate is in contact ion pairs and 10 % (resp. 18%) in the form of aggregates.³¹ A similar behavior can be expected in DEC, where the static dielectric constant is even lower. Previous ^{35}Cl NMR measurement in THF solution with various LiClO_4 concentrations showed that the maximum of the NMR spectrum is slightly down-shifted (from 1008.1 to 1007.4 ppm) when the salt concentration increases from 0.05 to 2 mol L⁻¹, whereas the band significantly broadens.¹² The NMR line broadening while increasing the salt concentration is the signature of contact ion pairs $(\text{Li}^+, \text{ClO}_4^-)_n$ and is due to the fact that the perchlorate ion undergoes interactions which break the symmetry of the ion. In DEC solutions, the NMR measurements reported in Figure 1 show clearly the broadening of the bands with the LiClO_4 concentration, indicating a similar behavior to that in THF. Nevertheless, for a given concentration, the width of the NMR bands is even broader in DEC than in THF solutions (Figure 1 inset), indicating that the distribution of oligomers in DEC solutions is much larger. For a high concentration of the salt, the solution contains a distribution of different oligomers, $(\text{LiClO}_4)_n$. Considering that at a concentration of 0.1 mol L^{-1} of LiClO_4 in diethyl ether, all the lithium perchlorates are in the form of contact ion pairs,³¹ and that in DEC (that has a lower dielectric constant than diethyl ether), the ^{35}Cl NMR spectra obtained for the 0.05 and 0.1 mol L^{-1} concentrations are identical (also in non-

normalized NMR spectra, not shown here), it can then be assumed that for the four concentrations studied here (0.05; 0.1; 0.5 and 1 mol L⁻¹), no isolated perchlorate anion is present, the considered species being mainly neutral species. The presence of different oligomers at different concentrations for a given LiClO₄/DEC solution has then to be considered to understand the reduction reactions of solvated electron in pulse radiolysis measurements of these solutions. This distribution shifts to larger *n* value by increasing the salt concentration.

Picosecond pulse radiolysis experiments. Transient absorption spectra and kinetics are measured by using 7 ps electron pulse for neat DEC and for solutions with different concentrations of LiClO₄ (Figures 2 and 3). In all cases, just after the electron pulse, an intense and very broad absorption spectrum is observed mainly in NIR and its intensity increases monotonically until the detection limit in the near-infrared (1500 nm) (Figure 3). This broad absorbance band was previously attributed to the formation of the solvated electron in DEC (denoted here e_{DEC}⁻).³² However, the kinetics at different wavelengths indicate that other species are present after the electron pulse (Figure 3, insets). According to the observations reported in Figures 2, 3 and 4, the following trends can be underlined:

1 –The decay of the solvated electron observed at 1400 nm is accelerated by increasing the salt concentration (Figure 2). At 1 mol L⁻¹ LiClO₄ concentration, the decrease of the signal is the fastest and is completed in less than 800 ps. For this wavelength, it is interesting to note that no residual absorption is detected at long times. Therefore, the observed absorbance at 1400 nm in our measurements represents only the kinetics of the solvated electron. It is known that the solvated electron in DEC absorbs in the NIR. The molar absorption coefficients of e_{DEC}⁻ at 1400 nm is ε_{1400 nm} (e_{DEC}⁻) = 2.8 × 10⁴ L mol⁻¹ cm⁻¹.³² If we consider that the solutions contain homogenously dissolved Li⁺ ions, then from the decay kinetics (Figure 2), the rate constant of the reaction between solvated electron and Li⁺ would be k ~ 1.3 × 10⁹ L mol⁻¹ s⁻¹. This value is too low, compared to that for a diffusion-controlled reaction between two opposite charged species in a low dielectric constant such as DEC solvent, but it corresponds to a rate constant between the solvated electron and a neutral species. The relatively slow decay confirms the non-dissociation of the salt in the solution.

2 – The initial absorbance of the solvated electron observed at 1400 nm (Figure 2) decreases with the increase of salt concentration. The initial absorbance decreases by 10 % at the lowest (0.05 mol L⁻¹) and 40 % at the highest (1 mol L⁻¹) LiClO₄ concentration. That indicates that at the high concentrations the precursor of the solvated electron is scavenged and reacts with the species present in solution by an ultrafast process. This ultrafast reduction reaction is in competition with the solvation process of the excess electron.

3 – The decay of the absorption band does not follow the same rate at different wavelengths. To show the kinetic behavior of the different possible species involved in the mechanism, the absorbance decays at 450, 530, 780, 1100 and 1400 nm are presented in Figure 3, in the insets for neat DEC and four LiClO₄/DEC solutions. The decay is faster at 1400 nm than at 1100 nm and this latter is faster

than at 780 nm, and around 400 nm we can even observe an increase of the absorbance at longer time. These differences indicate that other species than the solvated electron are formed after the electron pulse and that they contribute to the transient absorption spectra.

4- It is known that the radical of DEC noted DEC(-H)[·] absorbs around 700 nm. In fact, in DEC solution with 0.5 mol L⁻¹ acetone, as it scavenges the solvated electron, it was reported that DEC(-H)[·] presents a broad absorption band around 600-1200 nm that decays markedly slower than the solvated electron.³² This absorption band is weak compared to that of the solvated electron and its contribution in the data analysis is very weak. As shown in Figures 3, the shape of the absorption bands in the visible depends on the salt concentration indicating that in addition to the solvated electron and the radical DEC(-H)[·], other species are absorbing. In the absence of knowledge on the extinction coefficients of the different species, the G × ε products are compared for neat DEC solution and for those obtained in the presence of 0.05, 0.5 and 0.1 M LiClO₄ at three different times (20 ps, 500 ps and 1 ns) after the electron pulse (Figure 4). In the presence of LiClO₄, the shape of the absorption band is markedly different from that in neat DEC (Figure 4). At these three times, in the presence of 0.05 M LiClO₄, the absorption in the visible is always higher than in neat DEC solution. Meanwhile, the absorptions in 0.5 and 1 M LiClO₄ solutions are lower from 500 to 700 nm than in neat DEC solution, showing that the contribution of the solvated electron is less intense. It is also obvious that at longer time there is another band appearing at shorter wavelength than 450 nm in 0.5 and 1M LiClO₄ solutions.

Molecular simulations of the anions in DEC.

The kinetics and the transient absorption for a given dose bear witness of the presence of several species formed after the pulse: the solvated electron which absorbs strongly in the NIR, and other species absorbing at lower wavelengths. The shape of the absorption band of solvated electron in neat DEC does not change after the electron pulse showing that the solvation of electron in this solvent is faster than the time resolution (7 ps). The change of the amplitude of the absorbance at the lowest wavelengths suggests the presence of additional species. The reactivity of the solvated electron in DEC is completely different from that towards isolated Li⁺ ions for which (e_s[·], Li⁺) contact ion pairs are formed and detected.¹¹ The calculated absorption spectra of the oligomer anions (LiClO₄)_n^{·-} (*n*=1 - 4) in DEC are given in Figure 5. The maximum of the absorption band of the monomer was found at 1150 nm; and with increasing *n* of the oligomer, the absorption band becomes more and more spread with a high energy edge shifting more and more to the blue. As already discussed in our previous work,¹² these spectra are the most reliable spectra given by our method, namely: for the monomer the *homo*→*lumo* MPW1K/B3LYP spectrum, for the dimer the *homo*→*lumo*, *lumo*+1 pure B3LYP spectrum, and for the trimer and tetramer the full MPW1K/B3LYP spectra. From the results of the simulations in the two solvents it can be seen that going from THF to DEC (*i.e.* decreasing the dielectric constant from 7.4 to 2.8) results in a shift of all the absorption bands toward shorter

wavelengths. For the monomer, the band shifts from 1153 nm (in THF) toward 1144 nm (in DEC), for the dimer the bands shift from 1159 nm (in THF) toward 1052 nm (in DEC) and from 854 nm (in THF) toward 793 nm (in DEC) (Figure 5). From these calculations, it is also clear that globally the molar extinction coefficients of the maxima of the bands decrease when n increases.

Spectro-kinetic data analysis. As several transient species are present, the global analysis of spectro-kinetic data matrices was performed, including all data available for neat DEC and 0.05, 0.1, 0.5 and 1 mol L⁻¹ LiClO₄ concentrations in DEC. The 400 - 1400 nm wavelength range was selected and, to exclude signals with very low signal/noise ratios, we removed the signal around 780 nm corresponding to the fundamental of the probe laser, which is present in the supercontinuum. We imposed the absorption band of the solvated electron and the radical DEC(-H)[•] obtained independently from previous study.³² The SVD analysis of the global data matrix shows that in addition to the solvated electron and the DEC(-H)[•] there are 3 distinguishable components. The MCR-ALS analysis with 5 species results in a lack-of-fit (LOF) of 5.3 %. This analysis gives us the absorption band (Figure 6) and the kinetics of the species (Figure 7) involved in the mechanism. The recovered spectra contain a transient spectrum with a maximum around 400 nm, as we do not have access to lower wavelengths, another one absorbing at around 500-600 nm with another broad band around 1000 nm, and finally one absorbing mainly in the red with also a component around 1300 nm (Figure 6). It is interesting to note that we did not observe any species with a intense absorption band around 1100 nm (Figure 6). Considering the complexity of the solution before irradiation (see NMR results, Figure 1), one does not have access to the concentration of each (LiClO₄)_n species. It is therefore impossible to estimate the molar extinction coefficients of the transients, except for the solvated electron. However, from the analysis it is found that by increasing the concentration, the absorbance is more and more shifted to the blue with a decrease of the amplitude in the red part of the absorption spectra. In absence of concentration information, pseudo-kinetic traces were calculated by integrating over the wavelength the spectro-kinetic contribution of each species to the data matrix (Figure 7). It is clear that the kinetics of each species depend strongly on the concentration of the salt in DEC solution. The data analysis shows that the decay of the solvated electron is accelerated by increasing the LiClO₄ concentration, as it was observed directly at 1400 nm (Figure 2) where only the solvated electron absorbs. The species absorbing in the red (from 560 to 720 nm) is always formed within the electron pulse. At low LiClO₄ concentration (0.05 M) a slow decay is observed for this species, and at high concentration this decay is accelerated. The species absorbing around 500-600 nm follows a slow decay at 0.05 M but at 1 M its formation is very fast. Finally, the species absorbing around 400 nm is slowly formed for the solution containing 0.05 M LiClO₄, its formation in not fully complete within our time window but for 1 M it is formed within 500 ps and then decays slowly.

By comparing the calculated spectra (Figure 5) with those deduced from pulse radiolysis measurements at different concentrations (Figure 6 and 7), we can state that, as no species with a

maximum around 1200 nm could be found, the anion monomer $(\text{LiClO}_4)^-$ is not formed in these experiments whatever the salt concentration. The data analysis show from the kinetics that the broad absorption band observed around 1100 nm is due to $(\text{LiClO}_4)_3^-$. In fact the absorption band of the monomer is expected to be very intense at 1200 nm, but in addition to the solvated electron, according to the simulation the only species absorbing noticeably in this range is $(\text{LiClO}_4)_3^-$ which has another absorption band between 500 and 600 nm. We already reported that even in THF solutions, the monomer anion is not very stable and that its auto-reduction occurs very efficiently. Moreover, according to the NMR measurement in DEC solution, the neutral species are more abundant in the DEC solutions and their aggregation is favored. Then, it is possible that the monomer LiClO_4 does not exist in DEC solutions. Moreover, the species absorbing around 500 - 800 nm is the anion dimer $(\text{LiClO}_4)_2^-$, as its absorption band deduced from the data analysis is very similar to that given by quantum calculations (Figures 5 and 6). It is interesting to note that the dimer is formed within the pulse and then it decays (Figure 7), confirming that the solutions contain $\text{Li}(\text{ClO}_4)_2$ before irradiation. The dimers are reduced by pre-solvated electrons and solvated electrons. The absorption band with a maximum around 600 nm is attributed to the anion trimer $(\text{LiClO}_4)_3^-$ (Figures 6 and 7). Noteworthy, the decay of the trimer is slower than that of the dimer. Finally, the species absorbing at shorter wavelength than 450 nm is the anion tetramer $(\text{LiClO}_4)_4^-$. At low concentration, it is formed within 500 ps and we can observe its formation up to 3 ns. We should point out that the very good agreement between the spectra deduced from the data analysis and the ones that are calculated, making the assignment of the species unambiguous (Figures 5 and 6).

Mass spectrometry results. Reaction mechanisms under irradiation in these non-polar media clearly exhibit special features. Knowing that LiClO_4 is unreactive towards ionizing radiation, it is interesting to check how this behavior can be affected in DEC. Therefore, the samples were irradiated at 100 kGy and HRMS experiments were performed to detect possible chlorinated species resulting from the degradation of the salt in DEC. HRMS experiments were performed using two different concentrations of DEC/ LiClO_4 ; 1 M and 0.1 M. In both cases, a non-irradiated sample was also analyzed. The comparison between the irradiated and non-irradiated samples gives an insight into the ions generated by irradiation (Figure 8). It is important to notice that there is no significant variation in the mass spectrum for the different experimental conditions mentioned in the experimental section as well as at different LiClO_4 concentrations. Therefore, only the results obtained with the molar LiClO_4 concentration are given below. In the molar DEC/ LiClO_4 system studied by HRMS in negative mode (Figures 8a-b), the spectrum is strongly dominated by the presence of the ion ClO_4^- detected at m/z 98.949 (not shown here). Interestingly, the main difference between the irradiated and the non-irradiated samples are the peaks detected at m/z 82.947/84.943 in the irradiated sample, as shown in Figures 8a-b. These peaks correspond to the ClO_3^- ion (theoretical masses at m/z 82.953/84.950). In the positive mode (Figures 8c-d), the most abundant generated ions are the $[\text{DEC}-\text{H}]^+$ and $[\text{DEC}-\text{Li}]^+$ detected at m/z 119.076 and 125.084, respectively (not shown here). In agreement with our previous

results,³³ most of the decomposition products detected for the DEC/LiClO₄ system arise from neat DEC. However, after irradiation, a new chlorinated decomposition product was recorded at *m/z* 181.112/183.091 (Figure 8d). It may correspond to the [C₈H₁₇O₂Cl+H]⁺ formula (theoretical *m/z* at 181.099/183.096) containing a chlorine atom that can only arise from degradation products of LiClO₄.

Discussion and concluding remarks

Lithium perchlorate is used in batteries and also in organic chemistry as a catalyst. The behavior of this salt in low polarity solvents is important to understand reaction mechanisms. According to the above results, it is clear that the DEC/LiClO₄ solutions contain several neutral species, and even large (LiClO₄)_n clusters. The distribution of these oligomers depends on the salt concentration and, by increasing the concentration, the size distribution shifts to larger *n*. From the broader NMR line in DEC than in THF, it can be claimed that the DEC solutions contain much more oligomers with larger *n* than in THF solutions. This can be explained by the lower dielectric constant of DEC as compared to that of THF. The reduction of the oligomers by solvated electrons form different transient anions. The monomer (LiClO₄)⁻ is not observed and the dimer (LiClO₄)₂⁻ is clearly found within the electron pulse around 800 nm. Compared to the results obtained for the same system in THF, the absorption bands of the anions are blue shifted. By increasing the concentration of the salt, then favoring the formation of larger oligomers in the solution, the absorption spectra of transient anions are blue shifted. The blue shift is explained by the fact that the additional electron in the anions is more and more bound by one, two, three and four Li⁺ cations. Figure 9 shows that the SOMO energy decreases with *n* increasing. At very high concentration, there is almost a total absence of transient species absorbing in the NIR besides the solvated electron, indicating that in DEC solutions the solutes are only under the form of large oligomers for which the reduced species absorb only weakly in the visible.

The kinetics also show that the species absorbing around 780 nm is the most abundant one even at high concentration. In fact, the absorption around 780 nm corresponds to the dimer and the simulations show that it has a more stability compared to other anionic oligomers explained in our previous work.¹² For the first time we observed new species such as (LiClO₄)₂⁻, (LiClO₄)₃⁻ and (LiClO₄)₄⁻ absorbing in the visible. The (LiClO₄)_{*n*}⁻ anions are metastable with respect to self-reduction and they decay by forming decomposition products of the perchlorate anions. It is worth noting that, these reactions are not possible when the ions are well separated in solution, as Li⁺ and ClO₄⁻ ions are known not to react under ionizing radiation. In the present work, the proof of the reactivity of (LiClO₄)_{*n*} species is given by mass spectrometry analysis of irradiated solutions. After irradiating the solutions, ClO₃⁻ is directly observed, which confirms that contrary to the case of polar solvents, for which LiClO₄ is dissociated, in a low polarity solvent an unstable anion, (LiClO₄)_{*n*}⁻ is formed that can then react by forming ClO₃⁻. In that case, Li⁺ plays the role of a catalyst for the dissociation of ClO₄⁻.

The second indirect proof for the reactivity of ClO_4^- is the presence of a chlorinated species, such as $[\text{C}_8\text{H}_{17}\text{O}_2\text{Cl} + \text{H}]^+$ observed after irradiation of the DEC solutions containing perchlorate salt. The presence of such a compound also suggests the dissociation of perchlorate anions. The present work highlights then that low polarity solvents can induce a specific and unexpected reactivity.

Acknowledgements

This work was supported by a public grant from the “Laboratoire d’Excellence Physics Atom Light Mater” (LabEx PALM) overseen by the French National Research Agency (ANR) as part of the “Investissements d’Avenir” program (reference: ANR-10-LABX-0039). Financial support from the national FT-ICR network (FR 3624 CNRS) for conducting the research is also gratefully acknowledged. We thank Jean-Philippe Larbre and Pierre Jeunesse for their help during the experiments at ELYSE, and Jean-Marie Teuler for assistance in the use of GIBBS code. The authors want also to thank Vincent Steinmetz for his help in the HRMS experiments. Jean-Pierre Baltaze is gratefully acknowledged for the NMR experiments.

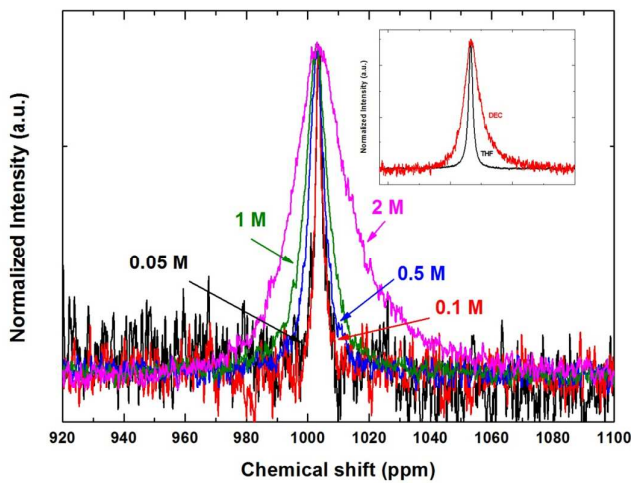


Figure 1. ^{35}Cl NMR spectra of DEC/LiClO₄ solutions at various LiClO₄ concentrations: 0.05 M (black), 0.1 M (red), 0.5 M (blue), 1 M (green) and 2 M (pink). Inset: comparison between the signals obtained for a 2 M LiClO₄ concentration in DEC (red curve) and in THF (black curve). To allow the comparison, the spectra have been shifted and normalized.

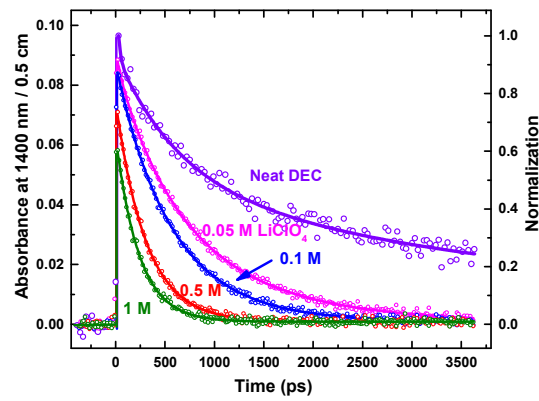


Figure 2. Kinetics of transient absorption in neat DEC and LiClO₄/DEC solutions at 0.05, 0.1, 0.5 and 1 M concentrations after the picosecond electron pulse at 1400 nm (Dose is 51 Gy per pulse).

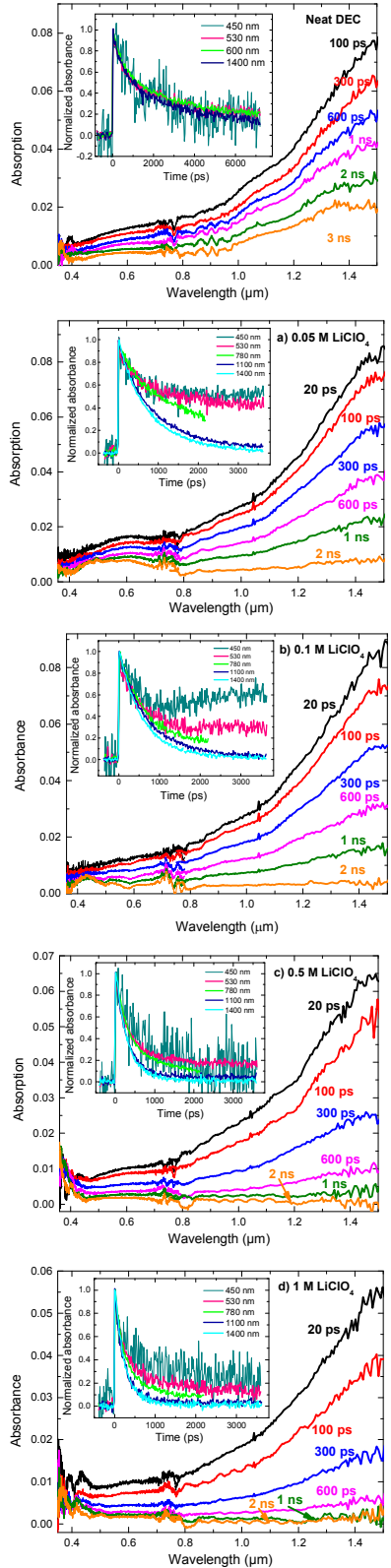


Figure 3. Transient optical absorption spectra in DEC/LiClO₄ solutions after the 7 ps electron pulse obtained in solution at concentrations of 0.05 M; 0.1 M, 0.5 and 1 M. The insets are the normalized kinetics at different wavelengths. The dose is 46 Gy per pulse and the optical path is 0.5 cm. The oscillations around 780 nm are due to the fundamental frequency of laser in supercontinuum. This part is removed for the data analysis.

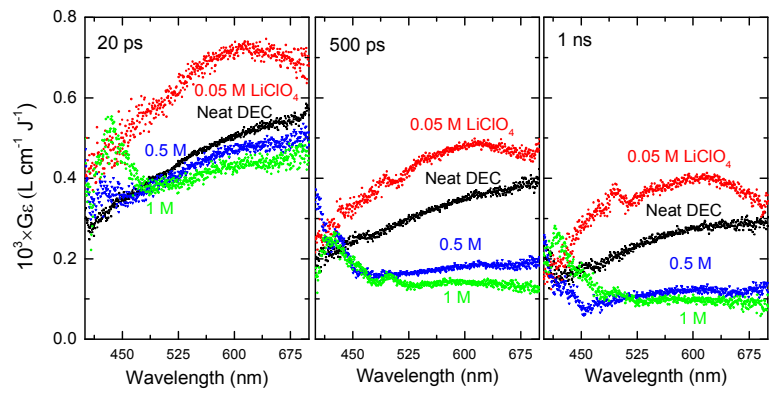


Figure 4. Comparison of the GE values at three different time for different solution in the visible range.

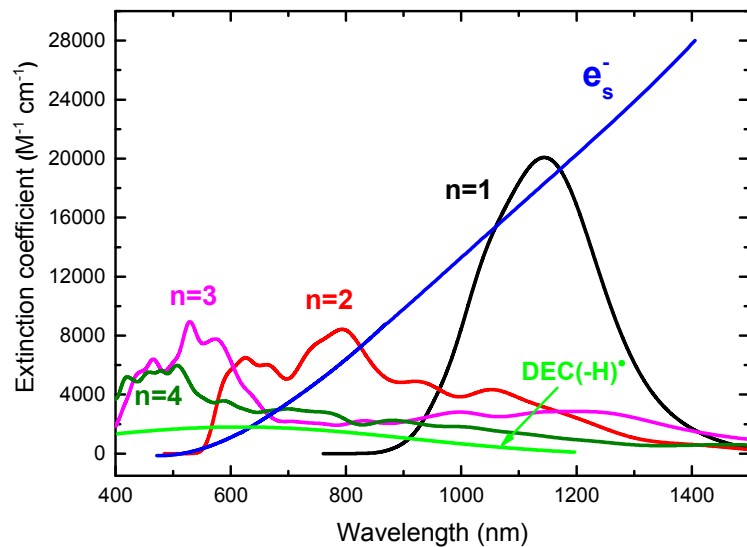


Figure 5. Calculated absorption spectra by MPW1K/B3LYP simulation method of the transient oligomers $(\text{LiClO}_4)_n$ ($n = 1 - 4$) in DEC. The experimental absorption band of the solvated electron and $\text{DEC}(\text{-H})^\bullet$ radical obtained by ps pulse radiolysis study of neat DEC are also reported.

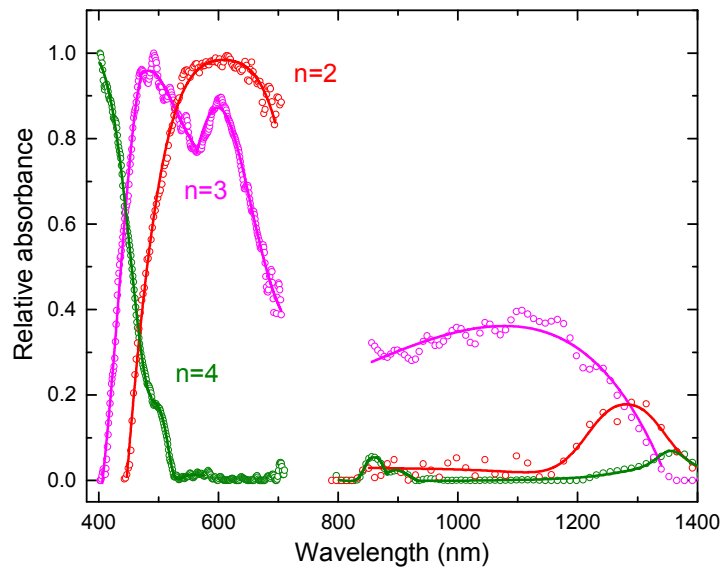


Figure 6. Normalized absorption spectra of transient radical anions in DEC obtained by global data (presented in Figures 3) analysis with the MCR-ALS method. The value of n is determined by comparing the results with those obtained with the quantum calculations (see Figure 5).

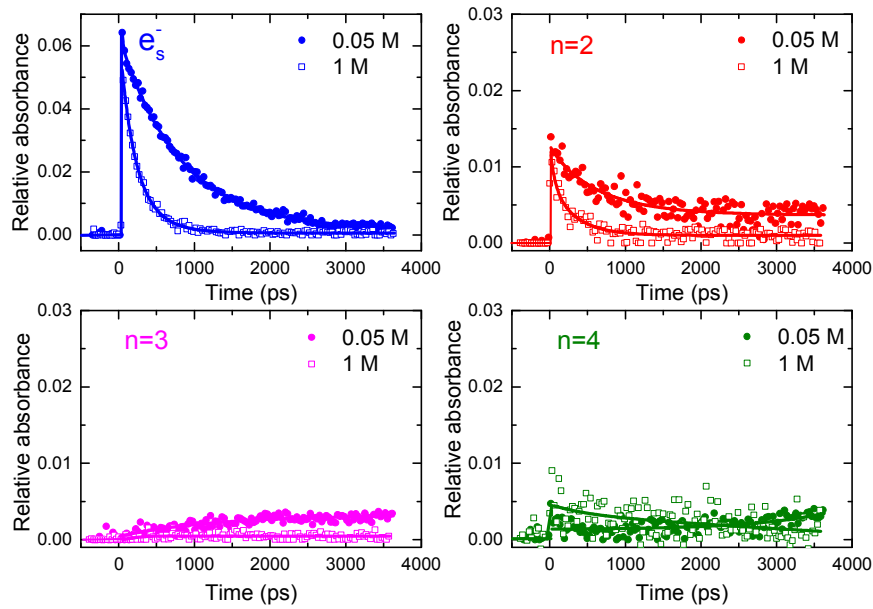


Figure 7. Kinetic traces from the MCR-ALS analysis of global data (presented in Figure 3) involving 4 species: the solvated electron and three anions $(\text{LiClO}_4)_n^-$ for concentrations of 0.05 M, and 1 M LiClO_4 in DEC. The value of n are deduced by comparing the spectra obtained by calculations (Figure 5) and experimentally (Figure 6).

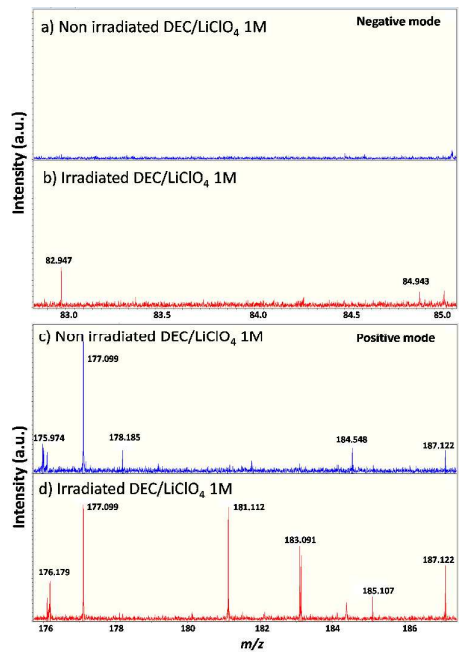


Figure 8. Mass spectra in the negative (a-b) and positive mode (c-d) of the a-c) non-irradiated DEC/LiClO₄ 1 M and b-d) DEC/LiClO₄ 1 M irradiated at a dose of 100 kGy.

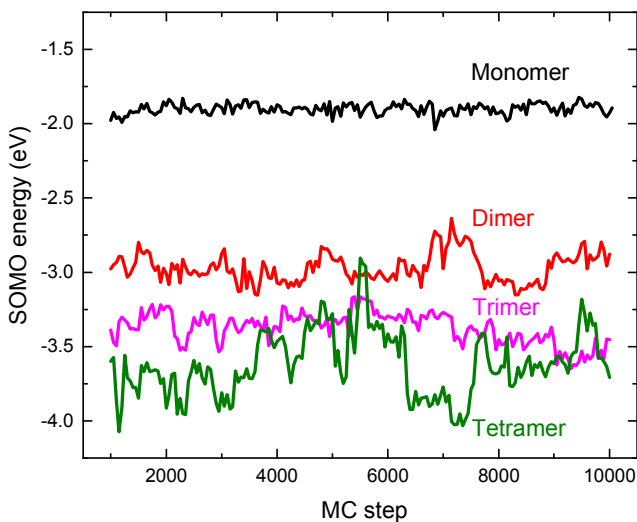


Figure 9. SOMO energy along the MC simulations for $(\text{LiClO}_4)_n^-$ with $n=1, 2, 3, 4$.

References

- (1) Hart, E. J.; Boag, J. Absorption Spectrum of the Hydrated Electron in Water and in Aqueous Solutions. *J. Am. Chem. Soc.* **1962**, *84*, 4090–4095.
- (2) *Solvated Electron, Advances in Chemistry Series 50*. Gould, R. F., Eds.; American Chemical Society Publications: Washington, D. C., 1965.
- (3) Baxendale, J. H.; Wardaman, P. Direct Observation of Solvation of the Electron in Liquid Alcohols by Pulse Radiolysis. *Nature*. **1971**, *230*, 449-450.
- (4) Chase, W. J.; Hunt, J. W. Solvation Time of the Electron in Polar Liquids. Water and Alcohols. *J. Phys. Chem.* **1975**, *79*, 2835-2845.
- (5) Delaire, J. A.; Delcourt, M. O.; Belloni, J. Solvated Electrons in Polar Solvents from Scavenging Rate Constants. *J. Phys. Chem.* **1980**, *84*, 1186–1189.
- (6) Holroyd, R. A. The Electron: its Properties and Reactions, in *Radiation Chemistry, Principles and Applications*. Rodgers M. A. J., Farhataziz Eds.; VCH, Weinheim, 1987; pp 201-235.
- (7) Buxton, G. V.; Greenstock, C. L.; Helman, W. P.; Ross, A. B. Critical-Review of Rate Constants for Reactions of Hydrated Electrons, Hydrogen-Atoms and Hydroxyl Radicals ($\cdot\text{OH}/\cdot\text{O}^-$) in Aqueous-Solution. *J. Phys. Chem. Ref. Data*. **1988**, *17*, 513–886.
- (8) Buxton, G. V.; Mulazzani, Q. G.; Ross, A. B. Critical-Review of Rate Constants for Reactions of Transients from Metal-Ions and Metal-Complexes in Aqueous-Solution. *J. Phys. Chem. Ref. Data*. **1995**, *24*, 1055–1349.
- (9) Bonin, J.; Lampre, I.; Soroushian, B.; Mostafavi, M. First Observation of Electron Paired with Divalent and Trivalent Nonreactive Metal Cations in Water. *J. Phys. Chem. A* **2004**, *108*, 6817–6819.
- (10) Bockrath, B.; Dorfman, L. M. Pulse Radiolysis Studies. XXII. Spectrum and Kinetics of the Sodium Cation-Electron Pair in Tetrahydrofuran Solutions. *J. Phys. Chem.* **1973**, *77*, 1002–1006.
- (11) Catterall, R.; Slater, J.; Seddon, W. A.; Fletcher, J. W. Correlation of Optical and Electron Spin Resonance Spectra for Alkali Metal Solutions in Ethylamine and Tetrahydrofuran. *Can. J. Chem.* **1976**, *54*, 3110–3113.
- (12) Ma J., Archirel, P.; Pernot P. ; Schmidhammer, U.; Le Caer, S.; Mostafavi, M. Identification of Transient Radical Anions $(\text{LiClO}_4)_n^-$ ($n = 1-3$) in THF Solutions: Experimental and Theoretical Investigation on Electron Localization in Oligomers. *J. Phys. Chem. B* **2016**, *120*, 773-784.

-
- (13) Ortiz, D.; Jiménez Gordon, I.; Baltaze, J.-P.; Hernandez-Alba, O.; Legand, S.; Dauvois, V.; Si Larbi, G.; Schmidhammer, U.; Marignier, J.-L.; Martin, J.-F.; et al. Electrolytes Ageing in Lithium-Ion Batteries: A Mechanistic Study from Picosecond to Long Timescales. *ChemSusChem* **2015**, *8*, 3605–3616.
- (14) Le Caér, S.; Ortiz, D.; Marignier, J. L.; Schmidhammer, U.; Belloni, J.; Mostafavi, M. Ultrafast Decay of the Solvated Electron in a Neat Polar Solvent: The Unusual Case of Propylene Carbonate. *J. Phys. Chem. Lett.* **2016**, *7*, 186–190.
- (15) Le Caér, S.; Rotureau, P.; Brunet, F.; Charpentier, T.; Blain, G.; Renault, J. P.; Mialocq, J.-C. Radiolysis of Confined Water: Hydrogen Production at a High Dose Rate. *ChemPhysChem* **2005**, *6*, 2585–2596.
- (16) Belloni, J.; Monard, H.; Gobert, F.; Larbre, J. P.; Demarque, A.; De Waele, V.; Lampre, I.; Marignier, J. L.; Mostafavi, M.; Bourdon, J. C. et al. ELYSE - A Picosecond Electron Accelerator for Pulse Radiolysis Research. *Nucl. Instrum. Meth. A* **2005**, *539*, 527–539.
- (17) Marignier, J. L.; de Waele, V.; Monard, H.; Gobert, F.; Larbre, J. P.; Demarque, A.; Mostafavi, M.; Belloni, J. Time-Resolved Spectroscopy at the Picosecond Laser-Triggered Electron Accelerator ELYSE. *Radiat. Phys. Chem.* **2006**, *75*, 1024–1033.
- (18) Schmidhammer, U.; Pernot P.; De Waele, V.; Jeunesse, P.; Demarque, A.; Murata, S.; Mostafavi, M. Distance Dependence of the Reaction Rate for the Reduction of Metal Cations by Solvated Electrons: a Picosecond Pulse Radiolysis Study. *J. Phys. Chem. A* **2010**, *114*, 12042–12051.
- (19) Schmidhammer, U.; El Omar, A. K.; Balcerzyk, A.; Mostafavi, M., Transient Absorption Induced by a Picosecond Electron Pulse in the Fused Silica Windows of an Optical Cell. *Radiat. Phys. Chem.* **2012**, *81*, 1715–1719.
- (20) Schmidhammer, U.; Jeunesse, P.; Stresing, G.; Mostafavi, M. A Broadband Ultrafast Transient Absorption Spectrometer Covering the Near-Infrared (NIR) Down to the Green. *Applied Spectroscopy*, **2014**, *68*, 1137–1147.
- (21) Muroya, Y.; Lin, M. Z.; Wu, G. Z.; Iijima, H.; Yoshi, K.; Ueda, T.; Kudo, H.; Katsumura, Y., A Re-evaluation of the Initial Yield of the Hydrated Electron in the Picosecond Time Range. *Radiat. Phys. Chem.* **2005**, *72*, 169–172.
- (22) Tauler, R. Multivariate Curve Resolution Applied to Second Order Data. *Chemom. Intell. Lab. Syst.* **1995**, *30*, 133–146.
- (23) Ruckebusch, C.; Sliwa, M.; Pernot, P.; de Juan, A.; Tauler, R. Comprehensive Data Analysis of Femtosecond Transient Absorption Spectra: A Review. *J. Photoch. Photobio. C* **2012**, *13*, 1–27.
- (24) Golub, G. H.; Van Loan, C.F. *Matrix Computation*, Second Edition. The John Hopkins University Press, London, 1989.
- (25) K.M. Mullen (2012). ALS: Multivariate Curve Resolution Alternating Least Squares (MCR-ALS). R package version 0.0.5. <http://CRAN.R-project.org/package=ALS> in the R language [R Core Team (2012). R: A language and environment for statistical computing. R Foundation for Statistical Computing, Vienna, Austria. ISBN3-900051-07-0, <http://www.R-project.org>.
- (26) Ungerer, P.; Tavitian, B.; Boutin, A., Applications of Molecular Simulation in the Oil and Gas Industry. Monte-Carlo Methods; Editions Technip: Paris, 2005
- (27) Marenich, A. V.; Cramer, C. J.; Truhlar, D. J. Universal Solvation Model Based on Solute Electron Density and on a Continuum Model of the Solvent defined by the Bulk Dielectric Constant and Atomic Surface Tensions. *J. Phys. Chem. B* **2009**, *113*, 6378–6396.
- (28) Frish, M. J. et al. Gaussian 09, Revision D.01; Gaussian, Inc., Wallingford, CT, 2013.
- (29) Becke, A. D. Density-Functional Thermochemistry. III The Role of Exact Exchange. *J. Chem. Phys.* **1993**, *98*, 5648–5652.
- (30) Lynch, B. J.; Fast, P. L.; Harris, M.; Truhlar, D. G. Adiabatic Connexion for Kinetics. *J. Phys. Chem. A* **2000**, *104*, 4811–4815.
- (31) James, D. W.; Mayes, R. E., Ion-ion Solvent Interactions In Solution. II Solutions of LiClO₄ In Diethyl Ether. *Aust. J. Chem.* **1982**, *35*, 1785–1792.
- (32) Torche, F.; El Omar, A. K.; Babilotte, P.; Sorgues, S.; Schmidhammer, U.; Marignier, J.-L.; Mostafavi, M.; Belloni, J., Picosecond Pulse Radiolysis of the Liquid Diethyl Carbonate. *J. Phys. Chem. A* **2013**, *117*, 10801–10810.

(33) Ortiz, D.; Steinmetz, V.; Durand, D.; Legand, S.; Dauvois, V.; Maître, P.; Le Caër, S. Radiolysis as a Solution for Accelerated Ageing Studies of Electrolytes in Lithium-Ion Batteries. *Nat. Commun.* **2015**, *6*, 6950.